Turkish Journal of Electrical Engineering & Computer Sciences

http://journals.tubitak.gov.tr/elektrik/

Research Article

Turk J Elec Eng & Comp Sci
(2020) 28: 2360 – 2374

doi:10.3906/elk-1904-152

Optimal SVC allocation in power systems using lightning attachment procedure optimization

Ayman AWAD[1,2], **Salah KAMEL**[1,3], **Heba YOUSSEF**[1], **Francisco JURADO**[2,*]
[1]Department of Electrical Engineering, Faculty of Engineering, Aswan University, Aswan, Egypt
[2]Department of Electrical Engineering, University of Jaén, Linares, Jaén, Spain
[3]State Key Laboratory of Power Transmission Equipment and System Security and New Technology, Chongqing University, Chongqing, P.R. China

Received: 19.04.2019 • **Accepted/Published Online:** 23.09.2019 • **Final Version:** 29.07.2020

Abstract: Flexible AC transmission systems (FACTS) technology is widely adopted and utilized to maintain the performance of power systems. However, the improvements of power system performance achieved by FACTS devices depend on the right sizing and allocation of such devices. For technical and economic considerations, a FACTS device's location and size should be selected very carefully in order to maximize its benefits to the power system. In this paper, the sizing and location of a static VAR compensator (SVC) are optimally determined using a new optimization technique called lightning attachment procedure optimization (LAPO). The optimal allocation of the SVC is determined regarding the improvement of voltage deviation index and the reduction of total active power losses. The system is optimized in two cases: once without SVC installation in order to find out the optimal settings of the system that achieve the objective functions, and another time with SVC installation to determine its optimum sizes and locations by which the required objective functions are achieved. Then the system performance is analyzed after optimization with and without SVC devices to show the impact of the optimum sizing and location of the SVC on the system. The study is validated using the standard IEEE 30-bus system, while the developed LAPO is performed by MATLAB M-Files and the system performance analysis in different cases is performed by NEPLAN software.

Key words: Power system optimization, voltage deviation index, power losses, FACTS, SVC, LAPO

1. Introduction

In the last few decades, due to the complexity of power systems, the continuous increase of load demand, and the limited capabilities of power systems to transfer power, there is a need to regulate power flow in power systems so that the voltage stability is improved, total active power losses are reduced, power flow over transmission lines is optimized, and the total power transferability of a system is enhanced so that the power system can serve more customers and deliver electric power with adequate quality. FACTS technology is used successfully for achieving such goals. Once it is installed in a power system, it has an excellent influence on the power system's performance. Depending on power electronics, it is capable of controlling the parameters of transmission lines, like voltage magnitude, phase angle (θ), line impedance (Z), and active and reactive power [1]. These capabilities enable the power flow to be regulated, and hence, to optimize the power transferability and quality. However, technically the size and location of a FACTS device's installation influence its effectiveness on a power system, and economically, it is important to maximize the benefits gained by the installation

*Correspondence: fjurado@ujaen.es

of such an expensive device. Thus, the installation of FACTS devices should not be randomized, and it is crucial to determine the best sizing and allocation of such an installation. Optimization techniques are used in many fields, and it is widely used in power system optimization, including optimal allocation and sizing of FACTS devices. Many contributions were introduced for detecting the optimal size and location of certain FACTS devices to achieve certain objective functions. These contributions were achieved by many optimization techniques, like particle swarm optimization (PSO) and its modifications [2–5], biography-based optimization (BBO) [5], moth flame optimization (MFO) [6], gray wolf optimization (GWO) [7], improved harmony search (IHS) algorithm [8], cuckoo search algorithm (CSA) [9], teaching learning-based optimization (TLBO) [10,11], the dragonfly algorithm (DA) [12], and the Pareto envelope-based selection algorithm [13]. Also, some of the contributions involving FACTS devices were achieved by hybrid techniques, like the hybridizations between artificial bee colony (ABC) and the gravitational search algorithm (GSA) in [14]; differential evolution (DE) and BBO, known as the hybrid DE-based BBO algorithm, in [15]; and chemical reaction optimization (CRO) with quasi-oppositional-based optimization in [16]. In this paper, the optimal sizing and location of the SVC in a power system is determined using a new optimization technique, known as lightning attachment procedure optimization (LAPO), in order to minimize the system's voltage deviation and total active power losses. The optimization process is applied to the system in three cases: 1) normal operation conditions, 2) sudden load increase, and 3) line branch out. For each case, the following steps are carried out: 1) system optimization process without SVCs to find the optimal settings that achieve the required objective functions, 2) system optimization process with SVC to find the optimal sizes and locations of SVC installations on the system that achieve the required objective functions, and 3) making a comprehensive analysis for the system in both cases to show the effectiveness of the optimized system with and without SVC. The effectiveness of optimization process on the system with and without SVC devices is validated using standard IEEE 30-bus system. The analyses on the system are performed by MATLAB and NEPLAN softwares. The contributions of this paper include: 1) determining the optimal size and location of SVC using the new optimization technique (LAPO), 2) improving the system loading ability and system response during abnormal conditions after implementing the SVC at its optimal allocation, 3) carrying out a comparative study to show the system's performance with and without SVC, 4) using the NEPLAN software tool to study the system loading ability based on the available PV curves analysis and to analyze the system response during abnormal conditions such as sudden load increase and branch outage, 5) validating the proposed algorithm using the standard IEEE 30-bus test system under different objective functions (minimization of the real power losses and voltage deviation index), and 6) utilizing a combination of two software tools (MATLAB and NEPLAN) to achieve the objectives of the paper. The rest of this paper is organized as follows: Section 2 describes the formulation of the optimization process, Section 3 discusses the LAPO optimization technique, Section 4 presents the analysis of the case study after optimization with and without SVC, and Section 5 gives the conclusion and future work.

2. Problem formulation

2.1. Objective function

In this paper, the main objective is to set the optimal location and compensation level of the SVC to minimize the real power losses and the voltage deviation index in the power systems. Therefore, the objective function is presented as a multiobjective function as represented in (1):

$$Min(F_t) = W_1F_1 + W_2F_2, \tag{1}$$

where F_1 represents enhancement of voltage deviation index by minimizing the maximum voltage stability indicator (L-index). The voltage stability index (L_{max}) was proposed by Kessel and Glavitsch to indicate system stability [17]. F_2 represents real power losses, while W_1 and W_2 consider weighting factors, where $w_1+w_2 = 1$. F_1 can be formulated as represented in (2):

$$F_1 = Min(L_{max}) = min(max(L_j)), j = 1, 2, ..., NPQ, \tag{2}$$

where NPQ is number of load buses. L_j is the voltage deviation index of bus j and it is calculated using (3):

$$L_j = |1 - \sum_{i=1}^{NPV} F_{ij}\frac{v_i}{v_j}|, \tag{3}$$

where NPV is number of voltage buses, v_i is the voltage of the ith generator bus, and v_j is the voltage of the load bus. F_{ij} can be obtained from the system Y_{bus} matrix as given in (4):

$$\begin{bmatrix} I_G \\ I_L \end{bmatrix} = \begin{bmatrix} Y_{GG} & Y_{GL} \\ Y_{LG} & Y_{LL} \end{bmatrix} \begin{bmatrix} V_G \\ V_L \end{bmatrix}, \tag{4}$$

where I_G, I_L are the complex currents and V_G, V_L are the complex voltages vectors at the generator and load buses. Y_{GG}, Y_{LL}, Y_{GL}, Y_{LG} are submatrices of system Y_{bus} by some manipulations:

$$\begin{bmatrix} V_L \\ I_G \end{bmatrix} = \begin{bmatrix} Z_{LL} & F_{LG} \\ K_{GL} & Y_{GG} \end{bmatrix} \begin{bmatrix} I_L \\ V_G \end{bmatrix}, \tag{5}$$

where F_{LG} and K_{GL} are partial inversions of Y_{GL} and Y_{LG}, and:

$$F_{ij} = [F_{LG}] = -[Y_{LL}]^{-1}[Y_{LG}]. \tag{6}$$

F_2 considers real power losses and can be calculated as given in (7):

$$F_2 = P_{loss} = \sum_{i=1}^{NTL} G_{ij}({V_i}^2 + {V_j}^2 - 2V_iV_jcos\delta_{ij}), \tag{7}$$

where G_{ij} is the transmission conductance, NTL is the number of transmission lines, and δ_{ij} is the phase difference of voltages.

2.2. Constraints

2.2.1. Equality constraints

The equality constraints represent the balanced load flow equations as given in (8) and (9):

$$P_{Gi} - P_{Di} = |V_i| \sum_{j=1}^{NB} |V_j|(G_{ij} \cos \delta_{ij} + B_{ij} \sin \delta_{ij}), \tag{8}$$

$$Q_{Gi} - Q_{Di} = |V_i| \sum_{j=1}^{NB} |V_j|(G_{ij} \cos \delta_{ij} + B_{ij} \sin \delta_{ij}), \tag{9}$$

where P_{Gi} and Q_{Gi} are the generated active and reactive power at bus i, respectively. P_{Di} and Q_{Di} are the active and reactive load demand at bus i, respectively. G_{ij} and B_{ij} are the conductance and susceptance between bus i and bus j, respectively, and NB is number of buses.

2.2.2. Inequality constraints

The inequality constraints can be calculated as follows:

Generation constraints

$$V_{Gi}^{min} \leq V_{Gi} \leq V_{Gi}^{max}, i = 1, 2, ..., NG, \tag{10}$$

$$P_{Gi}^{min} \leq P_{Gi} \leq P_{Gi}^{max}, i = 1, 2, ..., NG, \tag{11}$$

$$Q_{Gi}^{min} \leq Q_{Gi} \leq Q_{Gi}^{max}, i = 1, 2, ..., NG, \tag{12}$$

where voltages of generators are locked between 0.95 pu and 1.1 pu, generated active power is locked between 25% and 100% of the capacity of each generator, and generated reactive power is locked between 0 and 5 MVAr for each generator.

Transformer constraints

$$T_i^{min} \leq T_i \leq T_i^{max}, i = 1, 2, ..., NT, \tag{13}$$

where the transformers' ratios are locked between 0.9 and 1.1.

SVC controllers constraints

$$Q_{Ci}^{min} \leq Q_{Ci} \leq Q_{Ci}^{max}, i = 1, 2, ..., NC, \tag{14}$$

where the capacities of SVCs added to the system are locked between 0 and 30 MVAr.

Security constraints

$$S_{Li} \leq S_{Li}^{max}, i = 1, 2, ..., NTL, \tag{15}$$

$$V_{Li}^{min} \leq V_{Li} \leq V_{Li}^{max}, i = 1, 2, ..., NPQ, \tag{16}$$

where V_i^{min} and V_i^{max} are given as 0.90 Pu and 1.05 pu, respectively.

3. Overview on LAPO

3.1. LAPO inspiration

The LAPO algorithm is a nature-inspired algorithm, which simulates the procedure of lightning attachment. The lightning attachment procedure algorithm was proposed recently by Nematollahi et al. [18]. In this algorithm both the upward and downward leaders are considered. This technique simulates five phases of lightning accessories: 1)Air collapse on the cloud. 2)The leader's downward movement towards the earth. 3)Fading branch. 4)Ascending and spreading from the ground . 5)The final jump. These procedures are illustrated as following:

3.1.1. Phase 1: Air collapse on the cloud

The cloud can be divided into three parts, where in the bottom of the cloud there is a large quantity of negative charges, and in the upper part there is a large quantity of positive charges, and besides the negative charges in the bottom there is a small quantity of positive charges. A breakdown occurs between positive and negative charges when these quantities increase. After the collapse occurs, lightning is formed by increasing the voltage gradient at the edge of the cloud and thus moving a large charge in the direction of the ground that are mostly negative charges.

3.1.2. Phase 2: The leader's downward movement towards the earth

When the air touches the cloud surface, the collapse occurs and the lightning moves towards the earth but does not move in a straight line. It changes direction from time to time. In the hemisphere there are many possible points for the next jump so that the next point is chosen randomly. However, it can be chosen on the basis of the highest point of the electric field between the line connecting the leader and the corresponding point. This is more likely to serve as the next jump.

3.1.3. Phase 3: Fading branch

There are many points for the next jump and thus a division occurs in the main charge of the upper branch, and new branches appear. Also, these new branches are divided, and so on. This process continues until there is a collapse of the air when the branch charge is less than the critical value ($1\ \mu C$), and therefore does not produce more new branches.

3.1.4. Phase 4: Ascending and spreading from the ground

The presence of a negative charge on the surface of the earth indicates the presence of a cloud resulting in the accumulation of positive charges. The rising leader begins to rise. As the electric field increases in sharp points and the air collapses, the rising leader is deployed in the air and approaches the descending leader and the nomination occurs and the upper branches are exposed.

3.1.5. Phase 5: The final jump

A final jump occurs when a rising leader reaches an upward leader, the point from which the rising leader begins is an eye-catching point, all other branches disappear in this case, and the charge of the cloud is naturalized through this channel.

3.2. Mathematical steps of proposed algorithm

3.2.1. Test points

A random number of populations is selected and considered as test points located in the cloud and the earth; some of these tests are light-up lightning points, and some of them are points where upward leaders begin. All test points are calculated as shown in (17):

$$Z^i_{trailspot} = Z^i_{min} + (Z^i_{max} - Z^i_{min})rand, \tag{17}$$

where Z_{min} and Z_{max} are the minimum and the maximum bounds of variables, and rand is a random variable of range between 0 and 1. The target function is calculated for all test points as given in (18):

$$F^i_{trailspot} = obj(Z^i_{trailspot}). \tag{18}$$

3.2.2. Determine next jump

The averages of all test points can be calculated as given in (19):

$$Z_{avg} = mean(Z_{trailspot}). \tag{19}$$

The values of fitness of these points can be calculated as given in (20):

$$F_{avg} = obj(Z_{avg}). \tag{20}$$

There are many possible jump points for the test point that the lightning can pass through, so a random jump point is determined between the population. For test point i, a random point j is chosen among the population ($i/ = j$). The lightning moves to point j if the average value is less than the fitness of point j; otherwise, lightning moves to another direction. This step is formulated mathematically as follows: If the fitness of potential point j is higher than that of average electric field:

$$Z^i_{trailspot(new)} = Z^i_{trailspot} + rand(Z_{avg} + Z^j_{potentialspot}). \tag{21}$$

If the fitness of potential point j is lower than that of average electric field:

$$Z^i_{trailspot(new)} = Z^i_{trailspot} - rand(Z_{avg} + Z^j_{potentialspot}). \tag{22}$$

3.2.3. Fading branch

The branch is maintained if the fitness function is better than the previous point; otherwise, it fades. This can be formulated in (23) and (24) as:

$$Z^i_{trailspot} = Z^i_{trailspot(new)}, if F^i_{trailspot(new)} < F^i_{trailspot}, \tag{23}$$

$$otherwise : Z^i_{trailspot(new)} = Z^i_{trailspot}. \tag{24}$$

3.2.4. Rising leader movement

As we explained earlier, all test points are considered as downward leaders and move downwards. Also in this step, each point will be considered as a leader ascending and moving upwards. The rising leader movement depends on the downward leader's charges, which are distributed mainly along the channel. This can be formulated in (25) as:

$$S = 1 - (\frac{n}{n_{max}}) \exp^{(-\frac{n}{n_{max}})}, \tag{25}$$

where n is number of iterations, n_{max} is the maximum number of iterations, and the next jump based on the channel charge and the next point is given in (26):

$$Z_{trailspot(new)} = Z_{trailspot(new)} + rand * S(Z_{min} - Z_{max}). \tag{26}$$

3.2.5. Final jump

When the upward leader collides with the downward leader, the lightning operation ends and the crash point is the striking point. Figure 1 shows the flowchart of LAPO.

4. Analysis of case study

As mentioned before, the system is analyzed in each case after optimization with and without SVC so that the effectiveness of the optimized system is determined. The analyses applied are: 1)Load flow to find out bus voltages. 2)PV curves to detect the maximum loading ability of the system. 3)Dynamic analysis to determine the impact of sudden incidents on the system, according to certain scenarios. The previous steps are applied to the system after optimization in each case. In this section, the results of the optimization process and analyses are presented, and the scenarios applied to the system are: 1)Normal case: where the system is optimized in its normal conditions, according to the objective functions. 2)Case of sudden load increase: it is supposed that the system loads increase by 10% for each bus, and the system is optimized in this condition according to the objective functions. 3)Case of line branch out: a scenario of fault that caused line 3 of the system to branch out, where the system is optimized in this condition according to the objective functions. These cases and analyses are applied to the system with and without SVC. Table 1 shows the results of the optimization process for each case, where the parameters of LAPO are population size = 20 and maximum number of iterations = 200.

4.1. System optimization without SVC

As shown in Table 1, the optimized settings for the system operation were obtained and the system is analyzed according to these optimal settings as follows.

4.1.1. Normal case

Starting with system optimization in the normal case, and according to the optimized settings given in Table 1, the analyses were carried out. The load flow indicates that the total active power losses of the system in this case (P_{Loss}) = 3.0961 MW, and the maximum voltage deviation index (L_{max}) = 0.1278. For indicating the maximum loading ability of the case, PV curves are applied, and the result is graphed in Figure 2.

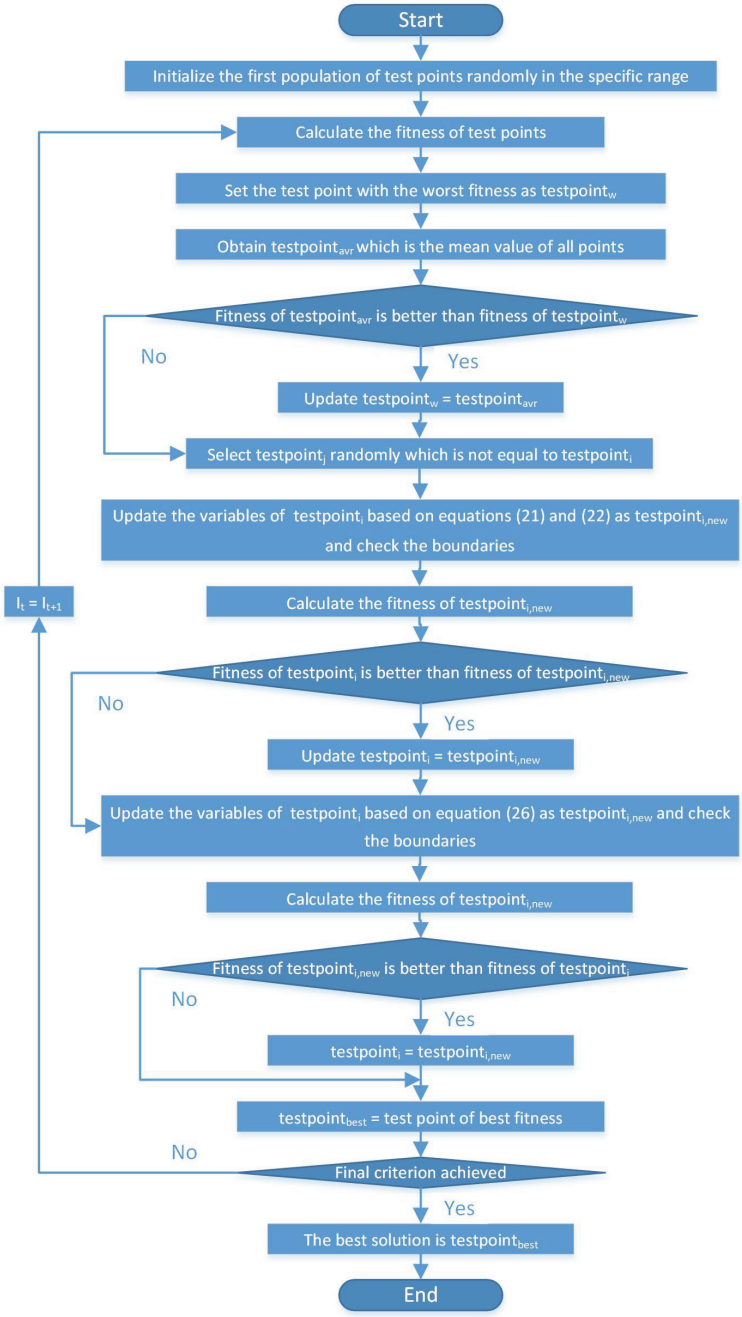

Figure 1. Flowchart of LAPO.

The graph in Figure 2 shows that the system's bus voltages start to descend below 90% when the total load exceeds 210%, and it collapses at 320%. As an evaluation step for the proposed optimization technique, a comparison is held between LAPO and other optimization techniques applied to the IEEE 30-bus system for solving the same objective functions mentioned in this paper [19]. Table 2 shows the values of total active power losses and voltage deviation index obtained by LAPO and other optimization techniques after system optimization.

Table 1. The system's optimized settings without SVC.

Element name	Location	Parameter	Parameter's value (pu)						
			Original case	Optimized case					
				Normal		Load increase		Line branchout	
				No SVC	With SVC	No SVC	With SVC	No SVC	With SVC
Generator 1	Bus 1	Bus voltage	1.06	1.0615	1.0615	1.069	1.068	1.053	1.067
Generator 2	Bus 2	Bus voltage	1.043	1.0573	1.0566	1.06	1.061	1.05	1.067
		Power generated	0.4	0.8	0.8	0.7997	0.8	0.7994	0.8
Generator 5	Bus 5	Bus voltage	1.01	1.0382	1.0845	1.037	1.09	0.999	1.009
		Power generated	0	0.499	0.499	0.499	0.499	0.4997	0.5
Generator 8	Bus 8	Bus voltage	1.01	1.0447	1.0447	1.042	1.044	1.042	1.042
		Power generated	0	0.349	0.35	0.35	0.35	0.3494	0.35
Generator 11	Bus 11	Bus voltage	1.082	1.0661	1.0594	1.1	1.069	1.014	1.085
		Power generated	0	0.3	0.3	0.299	0.3	0.3	0.3
Generator 13	Bus 13	Bus voltage	1.071	1.0492	1.0537	1.04	1.038	1.065	1.058
		Power generated	0	0.399	0.399	0.4	0.399	0.3978	0.4
Transformer 11	Buses 6,9	Tap ratio	0.978	1.0503	0.991	1.1	1.004	1.1	0.973
Transformer 12	Buses 6,10	Tap ratio	0.969	0.9	0.987	0.9	0.963	0.978	0.973
Transformer 15	Buses 4,12	Tap ratio	0.932	0.986	0.987	0.964	0.969	1.002	0.996
Transformer 36	Buses 27,28	Tap ratio	0.968	0.975	0.982	0.975	0.979	0.968	0.968
Shunt capacitor	Bus 10	Reactive power	0.19	0	0.0443	0.0021	0.0483	0.05	0.0484
Shunt capacitor	Bus 12	Reactive power	0	0.0497	0.00123	0.05	0.0499	0.0356	0
Shunt capacitor	Bus 15	Reactive power	0	0	0.0494	0.0488	0.036	0.499	0.0039
Shunt capacitor	Bus 17	Reactive power	0	0.05	0.0494	0.0486	0.0484	0	0.0414
Shunt capacitor	Bus 20	Reactive power	0	0.05	0	0.0119	0.0361	0.049	0.0425
Shunt capacitor	Bus 21	Reactive power	0	0.0496	0.05	0.05	0.0499	0.05	0.0499
Shunt capacitor	Bus 23	Reactive power	0	0.0495	0.0258	0.0453	0.0499	0.0004	0.0499
Shunt capacitor	Bus 24	Reactive power	0.043	0.05	0.0382	0.05	0.499	0.05	0.0135
Shunt capacitor	Bus 29	Reactive power	0	0.0178	0.0215	0.0248	0.0257	0.0017	0.0079

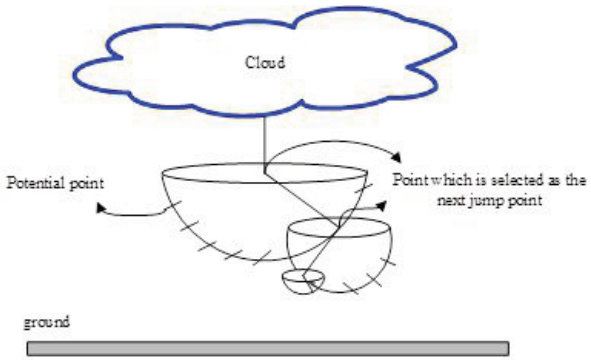

Figure 2. PV curves of system without SVC in normal case.

Table 2 shows that the results obtained by DE, MDE, and HMPSO are better than the results obtained by LAPO regarding voltage deviation index (L_{max}). However, it shows the superiority of LAPO regarding total active power losses of the system (P_{Loss}).

Table 2. Comparison of optimization results between LAPO and other techniques.

Optimization technique	DE	PSO	MDE	HMPSO	LAPO
P_{Loss}	4.8745	4.8753	4.8728	4.8723	3.0961
L_{max}	0.1276	0.1281	0.1275	0.1274	0.1278

4.1.2. Case of sudden load increase

In this case it is supposed that the loads increase in each bus by 10%. The optimization process obtained the settings previously shown in Table 1, and according to the optimized settings, the analyses were carried out, where the load flow indicates that the total active power losses (P_{Loss}) = 4.557 MW, and the maximum voltage deviation index (L_{max}) = 0.1423. PV curves indicate the maximum loading ability of the case, as shown in Figure 3. The graph shows that the system's bus voltages start to descend below 90% when the total load exceeds 205%, and it collapses at 310%.

On the other hand, the load increase scenario is applied to the system in this case to show the system's dynamic response, where the load increase incident took place at second 1. When it is applied, the system's response acts as shown in Figure 4, where the voltage of buses 13, 24, 26, and 30 are graphed. Figure 4 shows that the voltages of the buses are rippled for about 2 seconds, with a drop ranging from 0.002 pu to 0.008 pu.

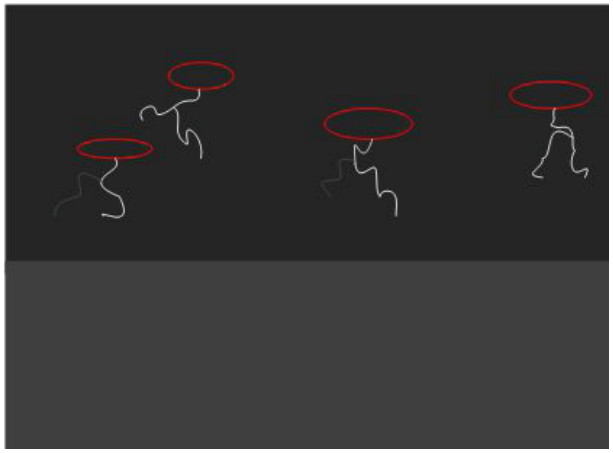

Figure 3. PV curves of system without SVC in case of load increase.

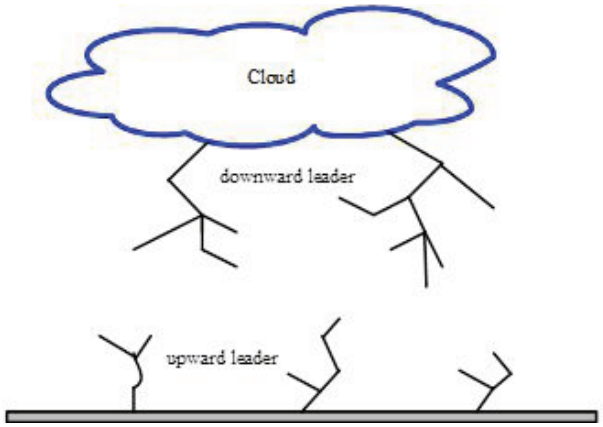

Figure 4. The optimized system's response to the load increase without SVC.

4.1.3. Case of branch outage

In this case, it is supposed that line 3 of the system –- the line that connects buses 2 and 5 –- branches out. According to the optimized settings shown in Table 1, the analyses were carried out, where the load flow indicates that the total active power losses (P_{Loss}) = 6.1803 MW, and the maximum voltage deviation index (L_{max}) = 0.1363. PV curves indicate the maximum loading ability of the case, as shown in Figure 5.

The graph in Figure 5 shows that the system's bus voltages start to descend below 90% when the total load exceeds 175%, and it collapses at 300%. On the other hand, the load increase scenario is applied to the system in this case to show the system's dynamic response, where the branch out took place at second 1.

When it is applied, the system's response acts as shown in Figure 6, where the voltages of generators' buses are graphed.

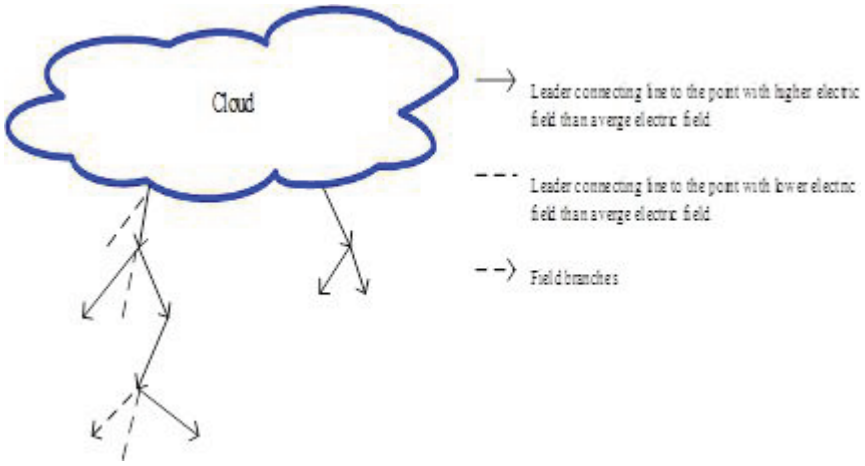

Figure 5. PV curves of system without SVC in case of branch outage.

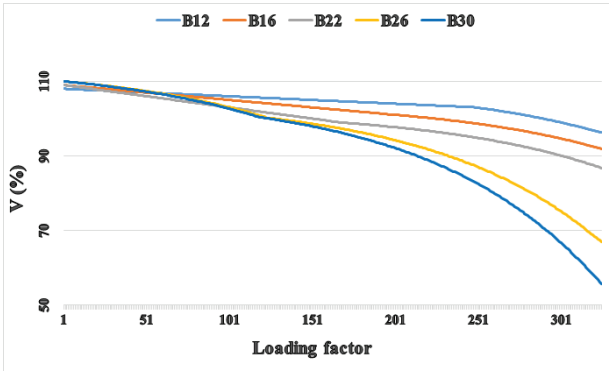

Figure 6. The optimized system's response to branch outage without SVC.

Figure 6 shows that the voltages of the buses dropped gradually from the start of the branch out until second 45, and then it severely dropped with a severe ripple in voltage value, which leads to total instability in the system.

4.2. System optimization with SVC

This time, the optimized settings of the system are obtained with the presence of SVC for the three cases, where the optimal sizing and location of SVC is also obtained by LAPO. The system is analyzed due to the optimized settings referred to in Table 1 and the SVC settings referred to in each case as follows.

4.2.1. Normal case

We start with system optimization in the normal case. In this case, two SVC devices are installed in the system in buses 19 and 26 with capacities of 4.0142 MVAr and 3.3137 MVAr, respectively, according to the optimization process. The load flow analysis indicates that the total active power losses (P_{Loss}) = 3.0935 MW,

and the maximum voltage deviation index (L_{max}) = 0.1258. For determining the maximum loading ability of the case, PV curves are applied, and the result is graphed in Figure 7.

The graph in Figure 7 shows great improvement in the system's maximum loading ability. The system's bus voltages start to descend below 90% when the total load exceeds 250%, and it collapses at 340%, while the values of voltage descending to below 90% with voltage collapse in the case of the normal system without SVC are 210% and 320% respectively.

4.2.2. Case of sudden load increase

Now the system is analyzed in case of load increase in each bus by 10% with the presence of the SVC, where the optimization process indicates two SVC installations in the system in buses 24 and 26 with capacities of 2.487 MVAr and 6.755 MVAr respectively. The load flow analysis shows that the total active power losses (P_{Loss}) = 4.515 MW, and the maximum voltage deviation index (L_{max}) = 0.138. PV curves indicate the maximum loading ability of the case, as shown in Figure 8.

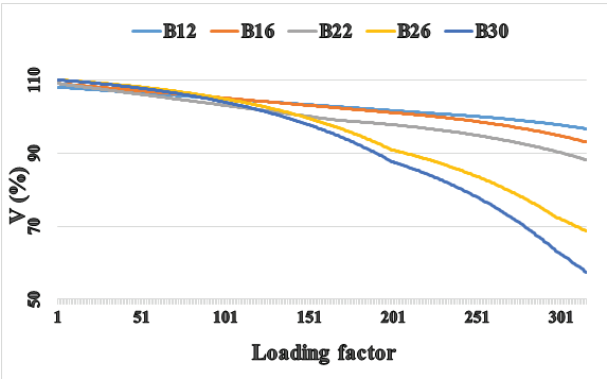

Figure 7. PV curves of system with SVC in normal case.

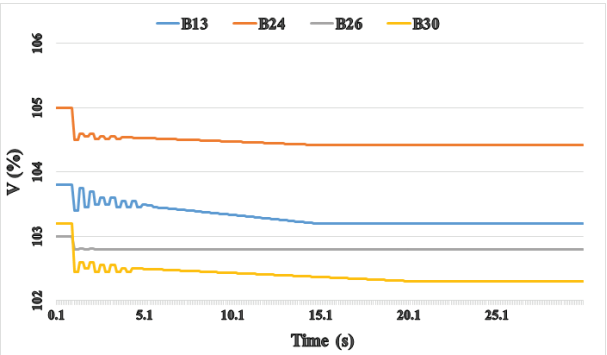

Figure 8. PV curves of system with SVC in case of load increase.

Figure 8 shows good improvement on the system's maximum loading ability, where the bus voltages start to descend below 90% when the total load exceeds 255%, and it collapses at 330%, while it starts to descend below 90% when the total load exceeds 205%, and it collapses at 310% when the SVCs were uninstalled. On the other hand, the load increase scenario is applied to the system in this case with SVC to show the system's dynamic response. The scenario is applied, and the system's response acts as shown in Figure 9, where the voltages of buses 13, 24, 26, and 30 are graphed.

Another improvement to the system with the SVC is shown in Figure 9. The figure shows that the voltages of the buses are slightly rippled and drop with a range that does not exceed 0.001 pu.

4.2.3. Case of branch outage

In this case, it is supposed that line 3 of the system -– the line that connects buses 2 and 5 –- branches out, and the optimization process with the SVC indicates four SVC installations in the system in buses 4, 7, 24, and 26 with capacities of 21.44, 9.904, 7.779, and 1.865 MVAr, respectively. The load flow indicates that the total active power losses (P_{Loss}) = 5.746 MW, and the maximum voltage deviation index (L_{max}) = 0.1258. PV curves indicate the maximum loading ability of the case, as shown in Figure 10.

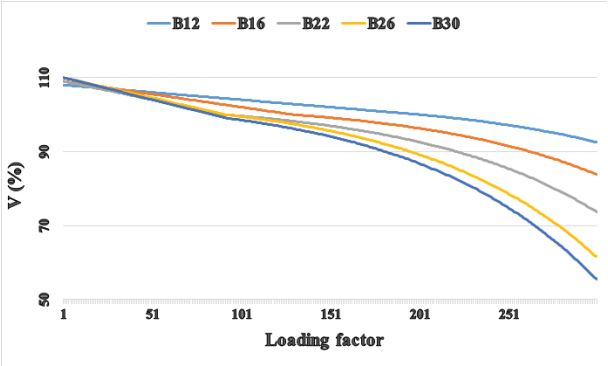

Figure 9. The optimized system's response to the load increase with SVC.

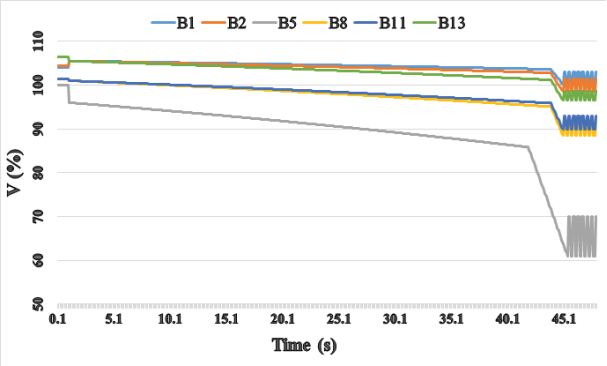

Figure 10. PV curves of system with SVC in case of branch outage.

The graph in Figure 10 shows that the system's bus voltages start to descend below 90% when the total load exceeds 225%, and it collapses at 320%, while it starts to descend below 90% when the total load exceeds 175%, and it collapses at 300% when the SVCs are uninstalled. Finally, applying the branch outage scenario to the system in this case to show the system's dynamic response, the system's response acts as shown in Figure 10 when applying this scenario, where the generators' buses voltages are graphed.

Figure 11 shows that the voltages of the buses slightly rippled after the branch out, while the voltage of bus 5 is significantly dropped from 1.009 pu to 0.978 pu. However, the total response of the system shows the stability of the system's voltage buses after the branch out.

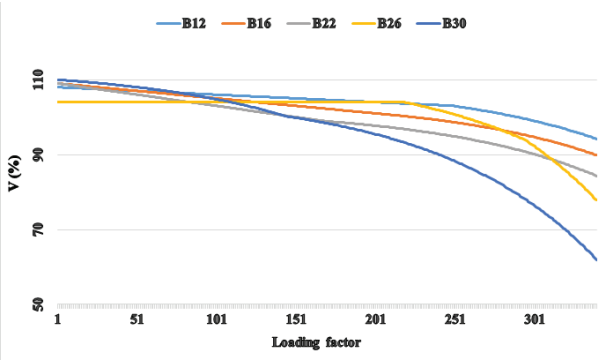

Figure 11. The optimized system's response to branch outage with SVC.

5. Conclusions

In this paper, the case study (IEEE 30-bus) is optimized in different cases using a new optimization technique (LAPO) in order to minimize the active power losses and voltage deviation, where the optimization process is carried out with and without SVC controllers. For each case, the optimized system's performance is analyzed and evaluated, and the impact of the optimization process on the system is shown with and without the SVC device, where the analyses are performed using MATLAB and NEPLAN software. The paper indicates an impressive performance for the optimized system with SVC, where the system's active power losses and voltage deviation index are less than those obtained in the case of the optimized system without SVC. Also, the maximum loading

ability of the optimized system with SVCs is improved compared to that of the optimized system without SVC, and finally, the dynamic response of the optimized system in each case is stabilized with SVC more than the optimized system without SVC. This study reflects the significant effect of the optimization process including FACTS devices – typically SVCs – compared to optimization excluding it. In the future, more studies should be carried out regarding optimal allocation and sizing of different FACTS devices, besides utilization of more recent optimization techniques for further power system improvement.

References

[1] Hingorani NG, Gyugyi L. Understanding FACTS: Concepts and Technology of Flexible AC Transmission Systems. 1st ed. New York, NY, USA: IEEE Press, 2000.

[2] Benabid R, Boudour M, Abido MA. Optimal location and setting of SVC and TCSC devices using non-dominated sorting particle swarm optimization. Electric Power Systems Research 2009; 79: 1668-1677.

[3] Mancer N, Mahdad B, Srairi K, Hamed M. Multi objective for optimal reactive power flow using modified PSO considering TCSC. International Journal of Energy Engineering 2012; 2: 165-170.

[4] Alvarez MS, Rodriguez CD, Jayaweera D. Optimal planning and operation of static VAR compensators in a distribution system with non-linear loads. IET Generation, Transmission and Distribution 2018; 12: 3726-3735.

[5] Kavitha K, Neela R. Optimal allocation of multi-type FACTS devices and its effect in enhancing system security using BBO, WIPSO and PSO. Journal of Electrical Systems and Information Technology 2018; 5: 777-793.

[6] Ebeed M, Kamel S, Youssef H. Optimal setting of STATCOM based on voltage stability improvement and power loss minimization using Moth-Flame algorithm. In: 2016 Eighteenth International Middle East Power Systems Conference; Cairo, Egypt; 2016. pp. 815-820.

[7] Amin A, Kamel S, Ebeed M. Optimal reactive power dispatch considering SSSC using Grey Wolf algorithm. In: 2016 Eighteenth International Middle East Power Systems Conference; Cairo, Egypt; 2016. pp. 780-785.

[8] Ebeed M, Kamel S, Nasrat LS. Optimal siting and sizing of SSSC using improved harmony search algorithm considering non-smooth cost functions. In: 2017 Nineteenth International Middle East Power Systems Conference; Cairo, Egypt; 2017. pp. 1286-1291.

[9] Nguyen KP, Fujita G, Dieu VN. Optimal placement and sizing of Static Var Compensator using Cuckoo search algorithm. In: 2015 IEEE Congress on Evolutionary Computation; Sendai, Japan; 2015. pp. 267-274.

[10] Abdou AA, Kamel S, Jurado F, Abd-ElSattar S. Voltage stability maximization of power system using TLBO optimizer and NEPLAN software. In: 2017 Nineteenth International Middle East Power Systems Conference; Cairo, Egypt; 2017. pp. 1122-1127.

[11] Youssef H, Kamel S, Aly MM. Optimal allocation and size of appropriate compensation devices for voltage stability enhancement of power systems. In: 2018 International Conference on Innovative Trends in Computer Engineering; Aswan, Egypt; 2018. pp. 305-310.

[12] Vanishree J, Ramish G. Optimization of size and cost of static VAR compensator using Dragonfly Algorithm for Voltage Profile improvement in power transmission systems. International Journal of Renewable Energy Research 2018; 8: 56-66.

[13] Ahmed W, Selim A, Kamel S, Yu J, Jurado F. Probabilistic load flow solution considering optimal allocation of SVC in radial distribution system. International Journal of Interactive Multimedia and Artificial Intelligence 2018; 5: 152-161.

[14] Kumar V, Srikanth NV. Optimal location and sizing of Unified Power Flow Controller (UPFC) to improve dynamic stability: A hybrid technique. International Journal of Electrical Power and Energy Systems 2015; 64: 429-438.

[15] Begovic M, Kim I, Novosel D, Rohatgi A. Hybrid biogeography–based optimisation for optimal power flow incorporating FACTS devices. International Journal of Power and Energy Conversion 2015; 6: 63-84.

[16] Dutta S, Paul S, Roy PK. Optimal allocation of SVC and TCSC using quasi-oppositional chemical reaction optimization for solving multi-objective ORPD problem. Journal of Electrical Systems and Information Technology 2018; 5: 83-98.

[17] Kessel P, Glavitsch H. Estimating the voltage stability of a power system. IEEE Transactions on Power Delivery 1986; l: 346-354.

[18] Nematollahi AF, Rahiminejad A, Vahidi B. A novel physical based meta-heuristic optimization method known as Lightning Attachment Procedure Optimization. Applied Soft Computing 2017; 59: 596-621.

[19] Singh H, Srivastava L. Optimal VAR control for real power loss minimization and voltage stability improvement using Hybrid Multi-Swarm PSO. In: 2016 International Conference on Circuit, Power and Computing Technologies; Nagercoil, India; 2016. pp. 1-7.